Alba Anglada Núñez

Synthesis of polystyrene microspheres towards the new route of radiolabelling strategy

BACHELOR'S THESIS

Supervised by Dr. Maya Al-Sid-Cheikh

School of Chemistry, University of Edinburgh

Tutorised by Prof. Elena Fernández Gutiérrez

Departament de Química Física i Inorgànica, Universitat Rovira i Virgili

Bachelor's degree in Chemistry

Edinburgh

2025

Acknowledgements

Vull dedicar aquesta petita secció de la memòria a agrair a totes aquelles persones que, d'una manera o una altra, han estat al meu costat durant aquest llarg viatge i han contribuït a que aquest treball sigui una realitat aportant-me suport, ànims i motivació en els moments clau.

First of all, I would like to thank Dr. Maya Al-Sid-Cheikh and Prof. Elena Fernández Gutiérrez to supervise and mentor me during the development of this work. To Maya, for welcoming me into your group and for trusting me from the very beginning. For celebrating the success of my research, sometimes even more than myself, for the encouragement and guidance you gave me throughout every stage of this project and for reminding me more than one time that I am an incredible student. Your support has helped me gain greater confidence in myself. A l'Elena, per confiar en mi durant el procés de l'Erasmus i per donar-me consells sempre que he tingut dubtes.

Si ara mateix soc aquí és gràcies a tots els que, d'una manera o una altra, m'ajudeu a ser millor persona cada dia. A la meva família, per haver-me donat sempre tot el que he necessitat, per realment creure que jo soc capaç de fer tot el que em proposo i per no deixar-m'ho de repetir dia rere dia. Als meus pares, per preocupar-se per mi i ajudar-me en tot. Al Marc, per fer-me riure com mai, sempre seràs el meu confident. A la yaya, por cuidar siempre de mí y por poner alguna velita de vez en cuando. A la Nuri, per ser-hi sempre. I als meus tiets, per creure en mi.

A la Teresa, per haver aparegut a la meva vida fa ara una mica més d'un any i haver-ho capgirat tot. Per estar sempre al meu costat i donar-me suport incondicional, sobretot en els moments més durs d'aquesta etapa final. Que sempre em recordis lo orgullosa que estàs de mi em fa sentir molt més segura de mi mateixa.

Als amics del grau, al Joan, a la Clàudia, al Rubén i al Gabriel, per haver compartit mil moments de felicitat, rialles, nerviosisme i, fins i tot, dificultats que ens han fet créixer junts. Gràcies per ser una part fonamental d'aquest viatge, sense vosaltres aquest camí hagués estat molt més dur. A mis amigas, a Lucía, a Paula, a Ana, a Salma y a Alba, por haber estado siempre a mi lado, por las risas, las experiencias compartidas y los consejos que siempre me dais. A l'Aaron, pel recolzament mutu davant de totes les dificultats que hem anat superant. Estic convençuda que en aquesta nova etapa que comencem, continuarem creixent i avançant junts cap a tots els objectius que ens proposem.

To Fin, Hannah, Jules, Danie, Jonathan and Grace, for all the unforgettable experiences we have lived together and for making my time in Edinburgh truly worthy. Your friendship is, without a doubt, one of the best memories I'll take from the Erasmus. To Tayabba, for making me laugh even in the most stressful moments, and for always reminding me the good person I am. I truly enjoyed being your lab mate.

Finalment, m'agradaria fer una petita menció a totes aquelles persones que no apareixeu en aquest escrit però que també m'heu ajudat a seguir endavant durant aquests anys.

Moltes gràcies a tots.

Table of Contents

Abstract

Polystyrene microspheres of 1 and 10 microns were successfully synthesized by a two-step polymerisation method. Firstly, the seeds (Dn, 0.97 μm) were prepared via chain-growth free-radical dispersion polymerisation, with benzoyl peroxide as initiator in ethanol-water medium in the presence of poly(acrylic) acid as stabilizer. Secondly, in the presence of the monodisperse (Dw/Dn, 1.08) polystyrene seed particles, two alternative preparation strategies were evaluated differing in the phase, aqueous or organic, used to disperse the seed particles. In both, the seed dispersion was mixed with an ethanol-water solution dissolving styrene, BPO as initiator, and poly(vinyl) alcohol as stabilizer. By slow, continuous, addition of water at a rate of 2.88 mL/h into the mixture, the PS particles absorbed the styrene and swelled up to *ca*.10 μm. Despite multiple efforts to maintain size uniformity, a loss of monodispersity was observed. Nevertheless, the surface of the PS seed particles was successfully functionalised by UV irradiation under different exposure times.

Sinopsi

S'han sintetitzat amb èxit microesferes de poliestirè d'1 i 10 micres mitjançant un mètode de polimerització en dos passos. En primer lloc, les “seeds” (Dn, 0.97 mm) es van preparar seguint la polimerització de dispersió radical lliure per creixement en cadena, amb BPO com a iniciador en un medi d’etanol-aigua en presència de PAA com a estabilitzador. En segon lloc, en presència de les partícules monodisperses (Dw/Dn, 1.08) de “seeds” de poliestirè, es van avaluar dues estratègies de preparació alternatives diferents en la fase, aquosa o orgànica, utilitzada per dispersar les partícules. En ambdós casos, la dispersió es va barrejar amb una solució d'aigua-etanol dissolent monòmer d'estirè, BPO com a iniciador i PVA com a estabilitzador. Per l'addició lenta i contínua d'aigua a la barreja, les partícules van absorbir els monòmers S i es van inflar fins a 10 μm. No obstant això, malgrat els múltiples intents de mantenir la uniformitat de la mida, es va observar una pèrdua de la monodispersitat. Finalment, la superfície de les partícules de PS ha estat funcionalitzada amb èxit per irradiació UV en diversos temps d'exposició.

Graphical abstract

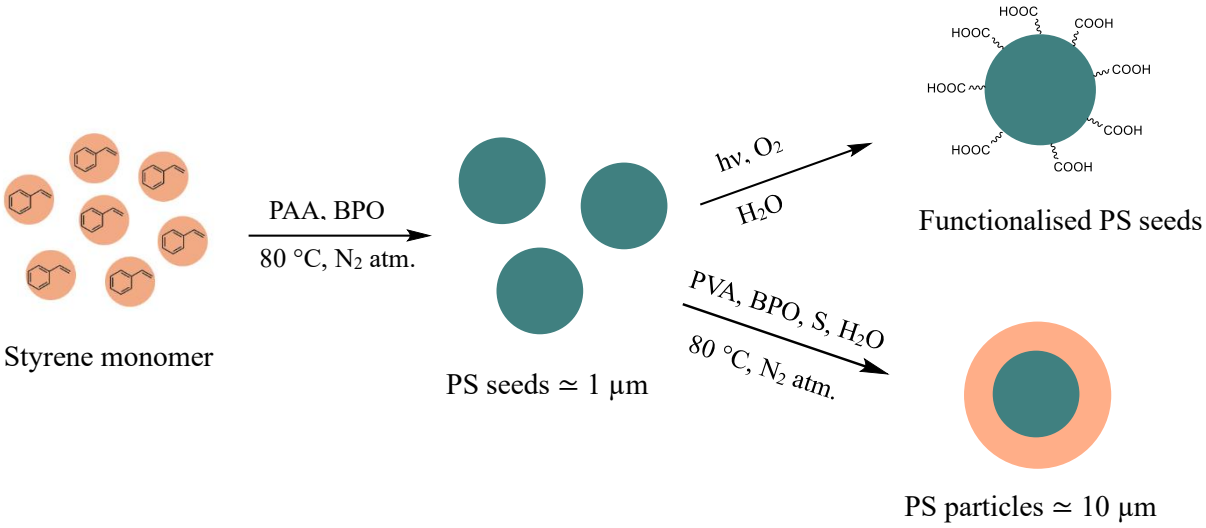

Acronyms and abbreviations

AIBN: 2,2'-azobisisobutyronitrile

BPO: benzoyl peroxide

°C: celsius degrees

CIE: carbon isotope exchange

DI: deionised

EtOH: ethanol

FT-IR: Fourier transform infrared.

MPs: microplastics

NMR: nuclear magnetic resonance

PAA: poly (acrylic acid)

PS: polystyrene

PVA: poly(vinyl) alcohol

RT: room temperature

S: styrene

SEM: scanning electron microscope

TGA: thermogravimetric analysis

US: ultrasound

UV: ultraviolet

1. Introduction

Polymers are macromolecules composed of repeating structural units; known as monomers. Natural polymers, such as cellulose, starch and lignin, have existed for millennia and play essential roles in biological systems. In contrast, synthetic polymers are relatively recent developments, but have gained considerable importance over the past few decades. Owing to the vast possibilities offered by chemical synthesis, an extensive variety of structural configurations can be achieved, leading to a broad spectrum of synthetic polymers with applications across virtually all industrial and technological sectors.[1] Examples of synthetic polymers are presented in Figure 1.

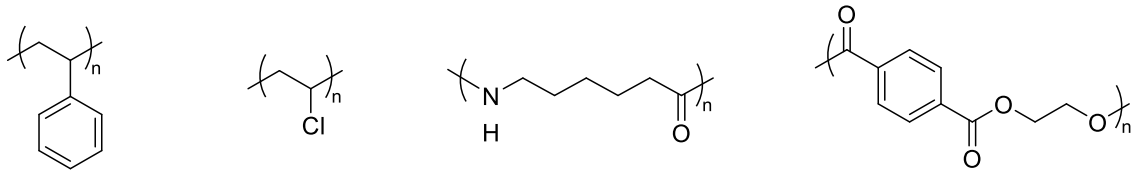

Polystyrene | Polyvinyl chloride | Nylon 6 | Polyethylene terephtalate

Figure 1. Examples of synthetic polymers.

Plastic litter in the environment primarily consists of polymeric materials designed for diverse applications. The most commonly found and environmentally present polymers are those widely used in manufacturing plastic products. When exposed to environmental weathering factors such as solar radiation, mechanical forces from ocean waves and chemical processes[2], these plastics undergo degradation and fragmentation. This degradation results in breakdown of larger plastic items into smaller solid particles, typically less than or equal to 5 mm in size, which are known as microplastics (MPs).[3]

Currently, MPs are ubiquitous and are found in every environment investigated by scientists: in the ocean, in Arctic snow and Antarctic ice, in table salt, in drinking water and beer, drifting in the air[4] or even inside the human body.[5] This highlights that MPs represent a global environmental pollutant problem, however, polymers also play an essential role in modern society. Their low cost, light weight, and high stability under thermal, chemical and mechanical stress in various environmental conditions make them widely used in for numerous applications,[6] including scientific research.

1.1. Polymerisation mechanisms

Synthetic polymers can be produced through three main types of polymerisation reactions: ring-opening polymerisation, step-growth polymerisation (also referred as polycondensation) and chain-growth polymerisation (or polyaddition).

Ring-opening polymerisation. In ring-opening polymerisation, polymers are formed by opening of cyclic monomers such as epoxides, lactones or lactams. These reactions require an initiator to start the polymerisation process, which can be anionic, cationic or coordinative depending on the system. An example of ring-opening polymerisation reaction is presented in Scheme 1.

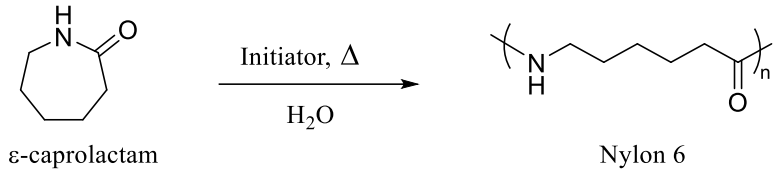

Scheme 1. Ring-opening reaction for the synthesis of Nylon 6.

Step-growth polymerisation (polycondensation). Polycondensation occurs when monomers containing reactive functional groups (such as acids, amides, alcohols or carbonates), undergo chemical reactions that form new bonds. These reactions often release small by-products, such as water or methanol. In step-growth polymerisation, monomers combine progressively to form oligomers, and high molecular weights are only achieved in the final stages of the process. An example of polycondensation reaction is shown in Scheme 2.

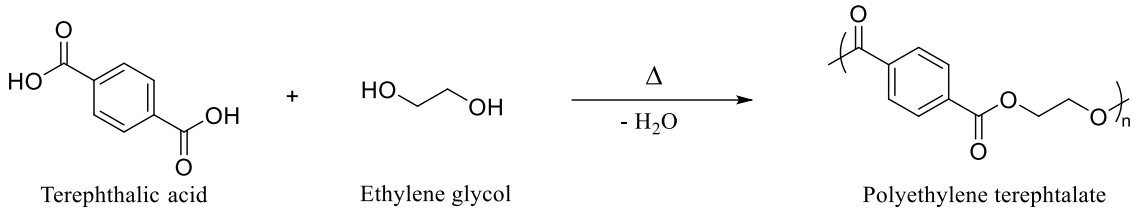

Scheme 2. Polycondensation reaction for the synthesis of polyethylene terephthalate.

Chain-growth polymerisation (polyaddition). In chain-growth polymerisation, monomers containing unsaturated bonds (double or triple bonds) react with an initiator that activate the monomer by opening the double bond, generating a reactive species. This species sequentially adds further monomer units to the growing chain. Chain-growth polymerisation proceeds through three distinct stages: initiation, propagation and termination. Depending on the initiator and reaction conditions, the mechanism may follow an anionic, cationic or radical pathway. Typically,

once the polymerisation is initiated, the propagation step is rapid, leading to a swift increase molecular weight. An example of polyaddition reaction is shown in Scheme 3.

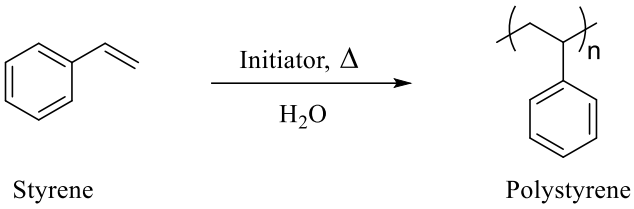

Scheme 3. Polyaddition reaction for the synthesis of polystyrene.

1.2. Polymer synthesis background

Among all the various mechanisms of chain-growth polymerisation, free radical polymerisation is the most widely employed due to its numerous practical advantages including adaptability, low cost, ease of operation, relatively simple initiation systems, and broad applicability. These features make it a preferred method in both industrial production and academic research.[7]

To synthesise monodisperse micron-sized polymer particles, several methods have been developed.[8] These include seeded emulsion polymerisation,[9] dispersion polymerisation,[10] microfluidic polymerisation,[11] precipitation polymerisation[12]. Among these methods, dispersion and seeding polymerisations are the most commonly utilised.[13]

Ugelstad et al.[14] demonstrated that dispersion seeded polymerisation, performed via a two-step swelling process with the assistance of a swelling agent, is effective for the preparation of polymer microparticles. Subsequently, Okubo et al.[10] proposed a modified monomer swelling technique for the synthesis of polymer seed particles larger than 5 μm. This approach eliminates the need for a swelling agent a simplifies the process to a single step. Okubo et al.[10] successfully synthesized 6.1 μm monodispersed polystyrene (PS) particles by swelling performed PS seed particles with an initial size of 1.8 μm. The PS seeds were prepared in an ethanol-water (80:20, v/v) medium using poly(acrylic acid) (PAA) as stabiliser, styrene (S) as monomer, and 2,2'-azobisisobutyronitrile (AIBN) as initiator. To produce swollen particles, the PS seed dispersion was combined with an ethanol-water (60:40, v/v) solution, additional styrene monomer, benzoyl peroxide (BPO) as initiator, and poly(vinyl alcohol) (PVA) as stabilizer. Subsequently, water was continuously and slowly added dropwise using a micro-feeder, allowing the PS particles to gradually absorb S monomer. This process was termed the “dynamic swelling method”.[10]

1.3. Labelling of Polymer Microparticles for Tracing Studies

In order to track and characterise the polymer microparticles, particularly for environmental or biomedical applications, various labelling techniques have been developed. This need arises due to the limitations of current analytical methods, which often struggle to detect microparticles at environmentally relevant concentrations within complex matrices such as biological tissues.[15]

Labelling techniques. Labelling techniques can broadly be categorised into extrinsic and intrinsic methods. Extrinsic labelling involves the attach of a marker to the polymer after synthesis. Common examples include metal doping[16] and fluorescence tagging.[17] In contrast, intrinsic labelling incorporates the label directly into the polymer structure, typically by introducing modified monomers during the polymerisation process. Isotopic labelling with deuterium (^{2}H), tritium[18] (^{3}H), ^{13}C and ^{14}C represent a widely applied example of intrinsic labelling.[19]

While it is true that both ^{3}H and ^{14}C labelling approaches have proven valuable insights into drug metabolism and distribution studies, ^{3}H labelling often suffers from limited metabolic stability due to the overlap between tritiation sites and metabolic transformation pathways. Conversely, ^{14}C-labelling offers superior stability, as the carbon backbone is less prone to metabolic cleavage. Although the synthesis of ^{14}C-labelled compounds can be complex and costly, ^{14}C radiotracers remain highly valuable in pharmaceutical research, particularly during the clinical development of drug candidates.

Two principal strategies have been developed in drug development for ^{14}C incorporation: the scaffolding approach and carbon isotope exchange (CIE). The scaffolding technique is an innovative intrinsic labelling method that incorporates ^{14}C isotopes at well-defined positions within the polymer backbone by constructing a labelled molecular framework from the very first steps of the synthesis. However, because labelling occurs at each synthetic step, incomplete reactions or purification losses result in the accumulation of radioactive waste and significant losses of costly ^{14}C-labelled material. Moreover, this approach is time-consuming and resource-intensive, highlighting the need for alternative strategies that are more sustainable, cost-effective, and time-efficient. In contrast, CIE offers a more direct approach by replacing existing ^{12}C atoms in functional groups with ^{14}C through isotope exchange reactions. This method has the potential to overcome many of the limitations associated with the scaffolding approach, by reducing radioactive waste, minimising synthetic steps, and improving both time and cost.

The CIE approach is a relatively recent development, and so far, its application has been primarily limited to small drug-like molecules. Most of the research efforts have focused on optimising the method for late-stage labelling of pharmaceuticals, where the introduction of ^{14}C can be achieved without the need to resynthesize the entire molecule from labelled precursors. This makes CIE

highly attractive for drug metabolism and pharmacokinetic studies. However, despite its advantages, the extension of CIE to larger macromolecular systems, such as polymers or nanoparticles, remains largely unexplored and presents new challenges in terms of reaction compatibility, functional group accessibility, and isotopic incorporation efficiency.

The CIE mechanism is illustrated in Scheme 4. In contrast to hydrogen isotope exchange, carbon-carbon isotope exchange is energetically more demanding due to the higher bond dissociation energy of C–C bonds. To facilitate the exchange, a metal catalyst is employed along with a $^{12}CO/^{14}CO$ gas mixture. Using suitably activated carboxylic acid derivatives under partial ^{14}CO atmosphere allows for efficient incorporation of the radiolabels.[19]

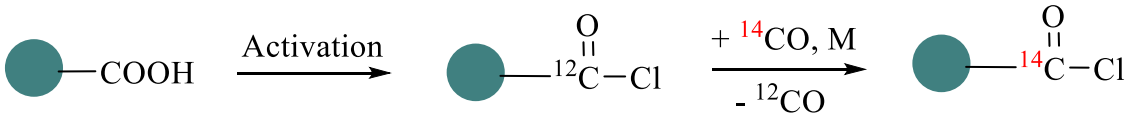

Scheme 4. Carbon isotope exchange graphical representation.

Based on these considerations, the aim of this project is to synthesise polystyrene (PS) microspheres of 1 and 10 µm in diameter via chain-growth free-radical dispersion polymerisation, followed by surface functionalisation to generate model particles suitable for subsequent carbon isotope exchange (CIE) radiolabelling. These functionalised particles are intended to be used in the detection and quantification of microparticles in environmentally relevant concentrations in several complex matrices such as biological tissues.

Goals

The main objective of the present study is to synthesize polystyrene microspheres of 1 and 10 microns by chain-growth free-radical dispersion polymerisation, with the use of an initiator capable of dissolving in the organic phase, to later produce model particles with developed functionalised surfaces to prepare carbon isotope exchange radiolabelling.

A distinctive feature of this work lies in the selection of the polymerisation initiator. While the majority of published protocols report the use of 2,2'-azobisisobutyronitrile (AIBN), this study employs benzoyl peroxide (BPO) as an alternative initiator. This deviation from conventional practice represents an innovative aspect of the synthesis approach, as BPO offers advantages related to its solubility in the organic phase and potential effects on particle size control, ultimately contributing to the advancement of radiolabelled microparticle development.

In order to achieve the main goal, the following specific objectives have been defined:

1. Synthesis of PS seed microspheres. To synthesise polystyrene seed microspheres of approximately 1 μm in diameter via free-radical dispersion polymerisation.
2. Swelling of seed particles. To apply a swelling procedure to the PS seed microspheres in order to increase their size to approximately 10 μm.
3. Control of polydispersity. To minimise the formation of new PS microspheres during the swelling step, thereby reducing the polydispersity of the final particle population.
4. Surface functionalisation. To subject the synthesised microspheres to UV irradiation in order to introduce surface functional groups suitable for subsequent radiolabelling.

2. Theoretical background

This project is composed of three different main steps. The first one is the synthesis of polystyrene seed microspheres of around 1-2 μm, the second one is the swelling of those seeds up to 10 μm, and the third one consists of functionalising the surface of the seed particles to later perform a labelling technique.

The method used to synthesize the particles is chain-growth free-radical dispersion polymerisation. Free-radical polymerisation is a type of polyaddition where the chain grows through the successive attachment of monomer units to a reactive radical site. This mechanism consists of three main stages: initiation, propagation and termination. Dispersion polymerisation is carried out in a solvent medium where styrene is initially soluble but polystyrene, the product, is not, so when the tiny polymer particles are created, they precipitate out of the continuous phase.

The reagents used in the reactions are styrene as monomer; BPO as initiator, which thermally decomposes to form free radicals, that are responsible for making the reaction begin; PAA, for the seeds, and PVA for the swelling, which both have the role of stabilizer, they adsorb onto the particle surface, providing steric or electrostatic repulsion and then, preventing agglomeration; and the solvent mixture is made of water and ethanol for both.

2.1. Reaction mechanisms

2.1.1. Seeds

For the seeds, the mechanism of the reaction is chain-growth free-radical dispersion polymerisation, which consists of three steps: initiation, propagation and termination.

Initiation

In the first step, the initiator, in this case BPO, thermally decomposes to create free radicals. These free radicals are highly reactive and can directly initiate the polymerisation by attacking the double bond of styrene monomers. The growing radical has now a terminal radical capable of adding more styrene monomers and continue in the propagation step. In the reaction it is used BPO as an initiator soluble in the organic monomer phase.

Scheme 5 displays the two initiation steps of the chain-growth free-radical dispersion polymerisation.

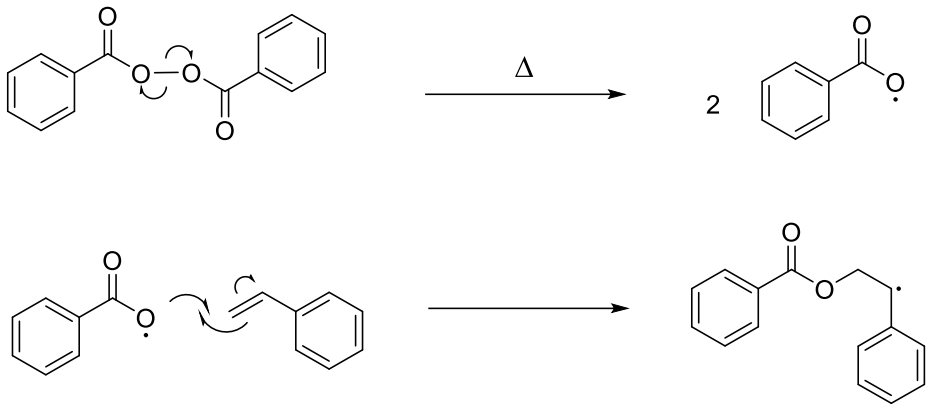

Scheme 5. Initiation steps of the chain-growth free-radical dispersion polymerisation using BPO.

Propagation

The reactive radical species continues to react and produces a chain reaction by sequentially adding styrene monomers, leading to the formation of an elongating polymer chain with a terminal radical.

As the chains grow, they become insoluble in the water-ethanol reaction medium, and they start to aggregate creating small polymer chunks. The stabilizer, PAA, adsorb onto the particle surface, providing steric or electrostatic repulsion and then, preventing further agglomeration. This is essential in dispersion polymerisation, where phase separation occurs during polymer growth.

In Scheme 6 it can be seen this propagation step of the chain-growth free-radical dispersion polymerisation.

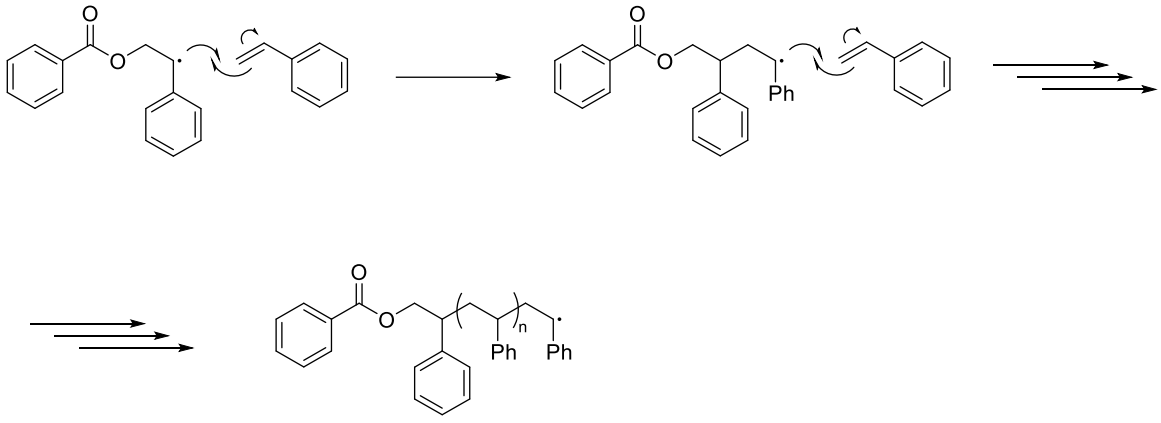

Scheme 6. Propagation step of the chain-growth free-radical dispersion polymerisation.

Termination

Chain growth can end via two main different mechanisms: termination by disproportionation, where a hydrogen atom is transferred from one radical to another and it leads into the formation

of one unsaturated and one saturated polymer end, or termination by combination, that occurs when two radical chains combine, neutralizing the active sites and creating one single final molecule of polymer with the initiator functional groups at both of the chain ends. In this case, termination by combination predominates because the benzyl radical is stabilized by resonance.[20]

Scheme 7 shows the termination mechanism step of the chain-growth free-radical dispersion polymerisation.

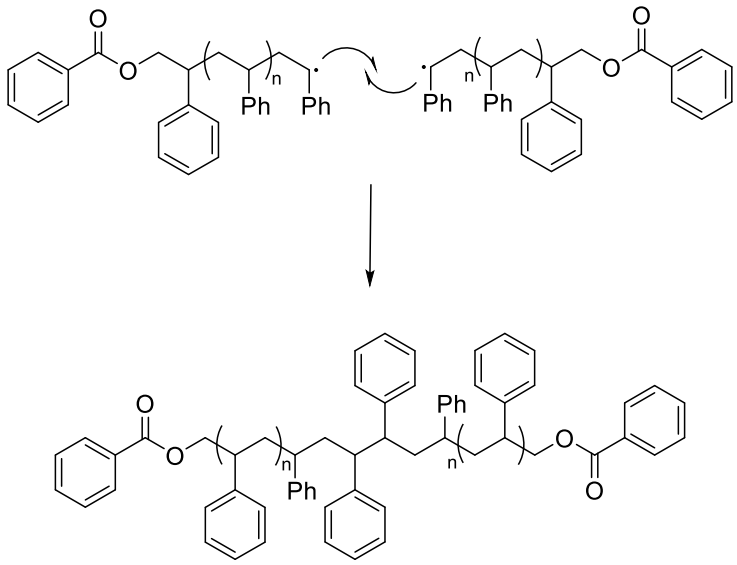

Scheme 7. Termination step of the chain-growth free-radical dispersion polymerisation.

2.1.2. Swelling

The swelling mechanism differs as larger microspheres are formed by expanding existing seed particles (1-2 µm in size), rather than creating new ones. Once the seed particles are added to the reaction medium, the styrene monomer diffuses into them, swelling the particles like tiny sponges as new layers of material accumulate. Upon increasing the temperature to activate the initiator, the polymerisation begins, solidifying the swollen particles into larger polystyrene microspheres.

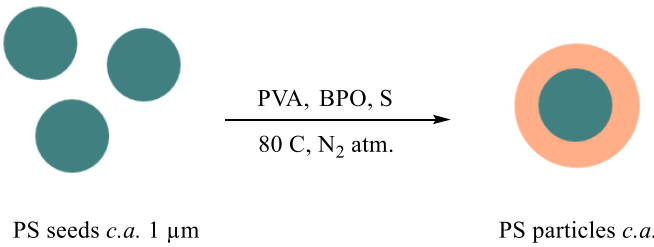

Figure 2. Swelling of the seed particles.

Figure 2 illustrates the swelling reaction of the PS seed particles. In the reagents, the green spheres represent the small PS seed particles. In the final swollen product, the green sphere serves as the core (the seeds), whole the surrounding orange layer represents the absorbed styrene monomer, which subsequently undergoes polymerisation to form the outer shell, resulting in a solid swollen polystyrene particle of around 10 µm.

2.1.3. Surface modification for the functionalisation of the particles

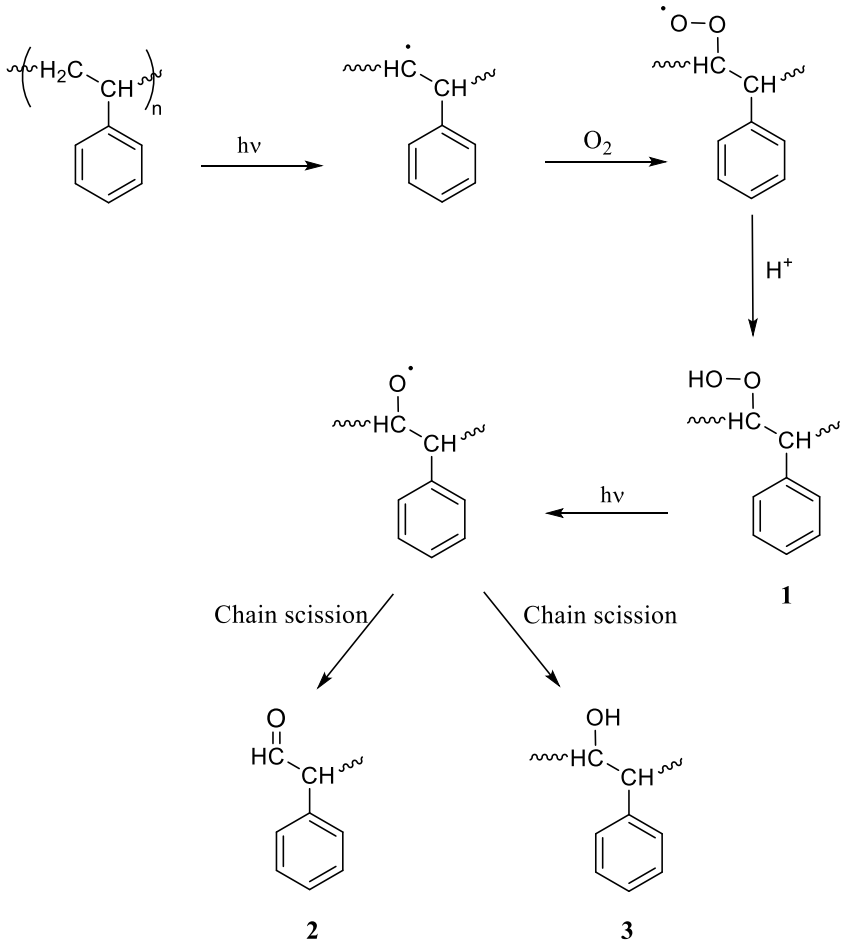

Scheme 8. Aging proposed mechanism of PS under UV irradiation.

The proposed mechanism of the functionalisation reaction is shown in Scheme 8. Once the PS particles are exposed to UV light, the bond in the benzylic position undergoes homolytic cleavage, resulting in the formation of a benzylic radical. This radical subsequently reacts with molecular oxygen (O_2) present inside the vial, leading to the production of peroxy radicals. As the particles are dispersed in water, the peroxy radicals can abstract hydrogen atoms from the surrounding environment (*i.e.* water), thus forming hydroperoxide groups (Scheme 8, molecule 1).

Hydroperoxides are typically expected to be the primary products formed after UV irradiation. However, due to their high photolability, they are also susceptible to further photochemical

degradation under continued UV exposure. This can lead to the generation of alkoxy radicals which, in the presence of air, may initiate chain scission events, which basically is a breaking in the polymer backbone.[21]

These degradations give rise to various oxidation byproducts, with aldehydes (Scheme 8, molecule 2) and alcohols (Scheme 8, molecule 3) being the most commonly observed. Therefore, this fact makes hydroperoxides key intermediates in the oxidation of polymers.[22]

3. Experimental part

3.1. Reagents and solvents

All the reagents used in this work were handled using laboratory coat, safety googles and nitrile gloves, inside a fume hood equipped with proper ventilation.

The commercially available reagents were used as received without any further purification. Distilled water was obtained from a MilliQ apparatus. Styrene (99%; Thermo scientific, GHS-02[a], GHS-07[b], GHS-08[c]; non-halogenated organic residues). Ethanol (99.8%; Thermo scientific, GHS-02, GHS-07; non-halogenated organic residues). Poly(acrylic acid) (PAA) (25 wt% solution in water: approx. M.W. 240,000; nitrogen flushed; Thermo scientific; non-halogenated organic residues). Benzoyl peroxide (BPO) (75%; Sigma-Aldrich, GHS-01[d], GHS-02, GHS-07, GHS-09[e]; solid residues). Polyvinyl alcohol (PVA) (87-89% hydrolysed, high molecular weight; Alfa Aesar; solid residues). Sodium nitrite (98%; Thermo scientific, GHS-03[f], GHS-06[g], GHS-09; solid residues). Copper (II) chloride dihydrate (99%; Thermo scientific, GHS-05[h], GHS-07, GHS-09; solid residues). Tetrahydrofuran (THF) (99.8%; Fisher Scientific, GHS-02[a], GHS-07[b], GHS-08[c]; non-halogenated organic residues).

3.2. Small polystyrene microspheres: Synthesis of polystyrene seed particles

Polystyrene particles, in size *ca.*1 μm, were produced by free radical dispersion polymerization procedure.[10] In a 50 mL round bottom flask, an aqueous solution of PAA (0.3968 g, 0,00165 mmol) was prepared in 10.7 mL of Milli-Q water and 25 ml of EtOH. This mixture forms the aqueous phase. All the reagent amounts, except for styrene, were measured by weight. The solution was N_2 purged for 5 minutes to establish an inert atmosphere, then placed in a Heat-On block and heated to 80 °C under stirring (180 rpm).

Once the solution reached the targeted temperature, styrene phase (4.4 ml, 38.4 mmol), containing dissolved BPO (0.0198 g, 0.082 mmol) as the radical initiator, was added to the flask via syringe. This addition introduced an immiscible organic phase, resulting in a biphasic reaction mixture.

[a] Hazard pictogram. Flammable.
[b] Hazard pictogram. Health Hazard/Hazardous to Ozone Layer.
[c] Hazard pictogram. Serious Health hazard.
[d] Hazard pictogram. Explosive.
[e] Hazard pictogram. Hazardous to the Environment.
[f] Hazard pictogram. Oxidizing.
[g] Hazard pictogram. Toxic.
[h] Hazard pictogram. Corrosive.

Polymerisation was allowed to proceed for 24 hours. The product was washed with Milli-Q water, vacuum filtered and dried at room temperature. The dried particles were stored in small vials, which were kept in a desiccator to prevent moisture uptake.

3.3. Large polystyrene microspheres: Swelling of the seed particles

The swelling of the PS seed particles (*ca.*10 μm in diameter) was carried out by adapting the procedure described by Okubo et al.[10]. Due to ambiguities in the original method, two alternative preparation strategies were evaluated, differing in the phase into which the PS seed particles were dispersed:

Dispersion into the aqueous phase

In a 50 ml round-bottom flask, an aqueous solution of PVA (0.015 g) was prepared in 4 ml of Milli-Q water and 7.6 ml of EtOH. PS seed particles (PS, 0.96 g; ethanol/water = 80:20) were sonicated for 5 minutes at room temperature to ensure complete dispersion and then added to the aqueous PVA solution.

Dispersion of PS seed particles into the organic phase

In this variation, the PS seed particles (PS, 0.96 g; styrene = 100) were pre-dispersed in the styrene phase instead of the aqueous phase, following the same sonication step prior to mixing.

For both methods, the resulting mixture was N_2 purged for 5 minutes to establish an inert atmosphere, then heated to 80 °C in a Heat-On block while stirring at 180 rpm. Once the temperature was reached, styrene (0.4 ml, 3.84 mmol) containing dissolved BPO (0.004 g, 0.02 mmol) as the radical initiator was added via syringe. Subsequently, Milli-Q water (40.0 g) was added dropwise at a rate of 2.88 ml/h with a push syringe.

After the addition of water, the mixture was stirred for an additional 12 hours to allow for swelling and polymerisation. The resulting product was isolated by centrifugation under varying solvent conditions, durations and speeds. The final particles were stored in small glass vials and placed in a desiccator to prevent moisture uptake.

In this polymerisation step, $NaNO_2$ or $CuCl_2$ were tested as polymerisation inhibitors to prevent the formation of new submicron-sized polystyrene particles. sodium nitrite was added in different reaction attempts either directly into the aqueous medium, together with the water during the swelling process or at the end of the reaction. Copper (II) chloride was only introduced at the end of the reaction.

3.4. Functionalisation of the seeds by using UV light

UV aging experiments were conducted using an EvoluChem PhotoRedOx Box photoreactor equipped with an 18 W lamp emitting at 365 nm. All experiments were carried out at 25 °C, with temperature maintained using a recirculating chiller.

A 0.1 % w/v suspension of PS seed particles was prepared in Milli-Q water in 7 mL glass vials. The suspensions were sonicated for 5 minutes at room temperature to ensure homogeneous dispersion. The vials were then placed in a rack holder, fully submerged in water bath, and exposed to UV light for specified durations.

After irradiation, each vial was removed at its designated time point, frozen overnight at –20 °C, and subsequently freeze-dried using a Labconco FreeZone 4.5 Liter Benchtop Freeze Dryer operating at –50 °C and 1 mbar vacuum. Samples were dried until complete removal of moisture was achieved.

3.5. Characterisation techniques

Scanning electron microscope

The shape and size of the particles were measured through a ThermoFisher Scientific Phenom Pure G6 Desktop scanning electron microscope (SEM), using a high-vacuum mode. For solid samples, a double-sided tape was placed on the top of the stub to which the sample adhered. Since the instrument operates under vacuum, air (or nitrogen) was sprayed over the sample to ensure that it was securely attached to the tape. For concentrated liquid samples, a serial dilution had to be done. A strip of parafilm was placed on the workbench inside the fume hood. First, five drops of 20 µL of deionised (DI) water and one drop of the concentrated sample were placed in a line. Using a micropipette, 5 µl of the concentrated sample were transferred into the nearest drop of DI water, and this process was repeated for all drops. Subsequently, 10 µl of the diluted sample were taken, placed on the stub, and left to dry at room temperature for several hours (at least 6 h) until the solvent was completely evaporated.

Fourier transform infrared spectroscopy

Fourier transform infrared (FTIR) spectroscopy was used to identify the functional groups from the samples. IR spectra were recorded on a ThermoFisher Scientific Nicolet™ Summit™ Fourier transform infrared (FTIR) spectrometer with a fast-recovery deuterated triglycine sulphate (DTGS) KBr detector. Both liquid and solid samples were measured with Everest Dimond ATR using blank as background. 16 scans were performed in all sample and background measurements.

To clean the crystal, it was used isopropanol. The spectrum was reported as % of transmittance (between -20 and 100) versus wavenumber values (between 4000 cm^{-1} and 500 cm^{-1}).

Thermogravimetric analysis

To investigate the thermal behaviour and kinetics of the samples by measuring their weight loss, it was utilized a Setline STA thermogravimetric instrument. The amount of sample employed was around 13 mg by using an 80 µL aluminum crucible, under inert nitrogen atmosphere. The heating rate was of 20 °C /min from 100 °C to 800 °C.[23]

4. Results and discussion

The objective of this work was to synthesise and characterise monodisperse polystyrene particles of approximately 1 μm and 10 μm in diameter, to serve as model particles. In addition, surface modification was performed to introduce carboxyl (COOH) functional groups as a first step to initiate the CIE approach for radiolabelling, enabling their future use in tracer studies and environmental fate experiments. The results presented below focus on evaluating the success of the synthesis protocols, assessing particle size distribution, morphology, surface functionality, and reproducibility of the procedure. After each reaction attempt, the resulting products were characterised using SEM, FTIR, and TGA to monitor the synthesis outcomes and verify whether the desired product had been obtained.

4.1. Synthesis of polystyrene seed particles

4.1.1. Size and morphology analysis

As it can be shown in Figure 3, the synthesis of the seed particles was successfully achieved as all of them have quite similar diameters, of about 1 μm (Dn, 0.97 μm; Dw/Dn, 1.08; Cv, 11 %). The uniformity and coefficient of variation calculations will be further discussed in subsequent sections to study the polydispersity of the seeds.

The procedure employed for the seed synthesis was a slight modification of the method reported by Okubo et al.[10] In this study, BPO was used as the initiator in place of AIBN, necessitating then an adjustment of the polymerisation temperature to 80 °C. After the reaction, the resulting particles were recovered by vacuum filtration, as the product exhibited effective retention in the filter.

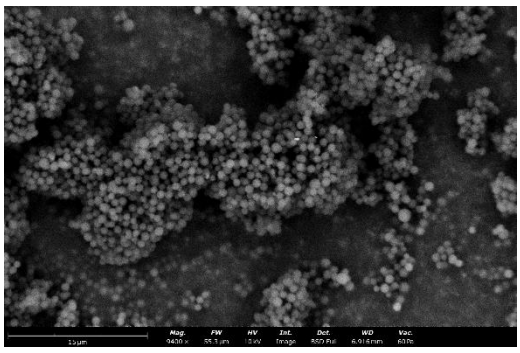

Figure 3. SEM image of PS seed particles.

4.1.2. Thermogravimetric analysis

Thermogravimetric analysis (TGA) was performed to the seeds sample to investigate the thermal stability and decomposition behaviour by measuring their weight loss. The TGA curve, which can be seen in Figure 4, was recorded by using 13 mg of initial sample and under a controlled heating rate from room temperature (25 °C) up to 800 °C. The spectrum reveals a very characteristic single-step degradation profile typical of pure polystyrene samples.

The spectrum was reported as furnace temperature (between 0 °C and 800 °C) versus TG values (between -10 mg and 0 mg).

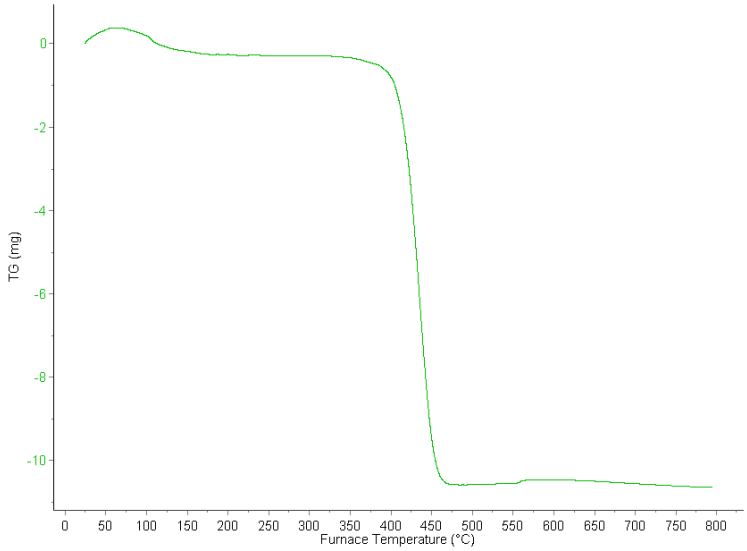

Figure 4. Thermogravimetric analysis (TGA) curve of the PS seed particles.

At the initial stage of the TGA spectrum, from room temperature to around 100 °C, the sample exhibits a small fluctuation in mass. This behaviour is mainly attributed to the instrumental stabilization, as the system requires a short period to reach thermal equilibrium to record an adequate spectrum. Importantly, there is no significant weight loss occurring in this region, within this temperature range, which can clearly indicate the absence of low-molecular-weight additives or volatile impurities, and therefore, it can confirm the purity of the sample.

The primary thermal event happens between 350 °C and 450 °C, which can be considered to be the major decomposition of the product as a sharp and substantial decrease in mass is observed. This significant fall corresponds to the thermal degradation of polystyrene, which is attributed to random chain scission and depolymerisation. Depolymerisation, which mainly yields volatile monomeric species such as styrene, is common in polystyrene samples due to its weak backbone stability. The onset of thermal degradation is approximately 350 °C and the process concludes around 450 °C, validating the sample identity and being consistent with literature-reported degradation temperatures for neat polystyrene.[23]

After 450 °C, the curve levels off, which means that the mass is stabilized, and no further significant weight loss is observed up to 800 °C. The low residual mass content (from 0 to approximately -10.5 mg from initial mass) suggests a complete thermal decomposition of the polymer under the experimental conditions in inert atmosphere of nitrogen and leaving negligible carbonaceous residue.

So, to sum up, the rapid and well-defined single-step curve of the weight loss indicates sample purity and homogeneous polymer composition. Therefore, the synthesis and the purification steps of the seeds from this work can be considered to be successful.

TGA was not performed on either the swelling products or the functionalised particles due to the insufficient quantity of sample available, making the analysis unfeasible.

4.2. Swelling of the seed particles

4.2.1. Size and morphology analysis

This second step of the reaction was carried out multiple times as the aim was not only to apply a swelling procedure to the PS seed microspheres in order to increase their size to approximately 10 μm, but also to control the polydispersity of the samples by minimising the formation of new PS microspheres during the swelling step, thereby reducing the polydispersity of the final particle population.

In this case, in contrast with the seed purification process, the purification method involved centrifugation. Initial attempts to use vacuum filtration resulted in significant product loss as the particles were not retained by the filter and went directly to the filtrate waste solution. Consequently, centrifugation was tested, and it was observed that it provided improved particle recovery. Based on these results, centrifugation was continued to use as the standard purification technique for all swelling attempts.

The first attempt was based on Okubo et al.[10] method, in which they claim to use an ethanol/water = 80:20, v/v mixture to disperse the PS seed particles. As shown in the SEM image in Figure 5, the reaction was unsuccessful, with almost no particles observed. The underlying reason for this failure may be related to insufficient stabilisation of the seed particles in the ethanol-rich medium, leading to aggregation or incomplete growth.

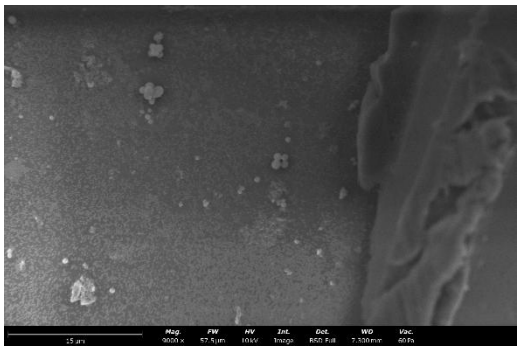

Figure 5. SEM image of the first swelling attempt.

In an effort to improve the reaction outcome, the seeds were subsequently dispersed directly into styrene, the monomer used for both swelling and polymerisation. The rationale behind this approach was that dispersing the particles directly into the styrene medium prior to swelling could enhance particle distribution, promoting a more efficient and uniform swelling process and ultimately facilitating the formation of swollen particles. As shown in Figure 6, this strategy resulted in the formation of particles with diameters in the range of 8-10 µm. However, a significant population of smaller particles is also visible in the image, indicating that the product is largely polydisperse. (Dn, 8.21 µm; Dw/Dn, 1.74; Cv, 59 %).

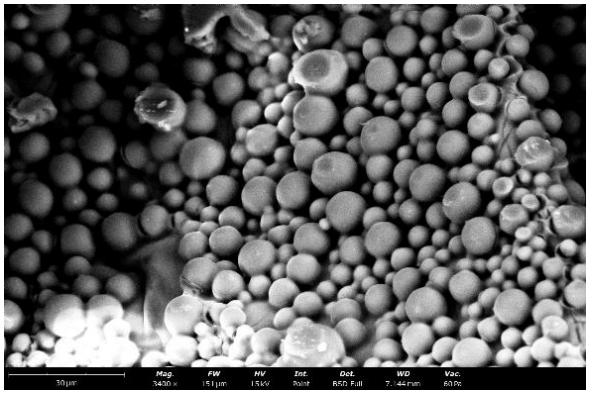

Figure 6. SEM image of swollen seed particles.

To reduce the polydispersity of the samples and to minimize the presence of smaller 2 µm particles, water-soluble inhibitors were introduced to supress the formation of new submicron-sized polystyrene particles. Two inhibitors were tested: sodium nitrite ($NaNO_2$) and copper (II) chloride ($CuCl_2$). Although the literature regarding the use of these inhibitors was unclear on the optimal concentrations and methods for quenching the reaction, sodium nitrite was added at three different stages of the reaction to evaluate its effect: (a) directly into the aqueous medium, (b) dropwise alongside the 40 mL of water, and (c) at the very end of the reaction, once it was completed and cooled down (Figure 7, a, b, c respectively). Copper (II) chloride was tested once, being introduced only at the end of the reaction (Figure 7, d).

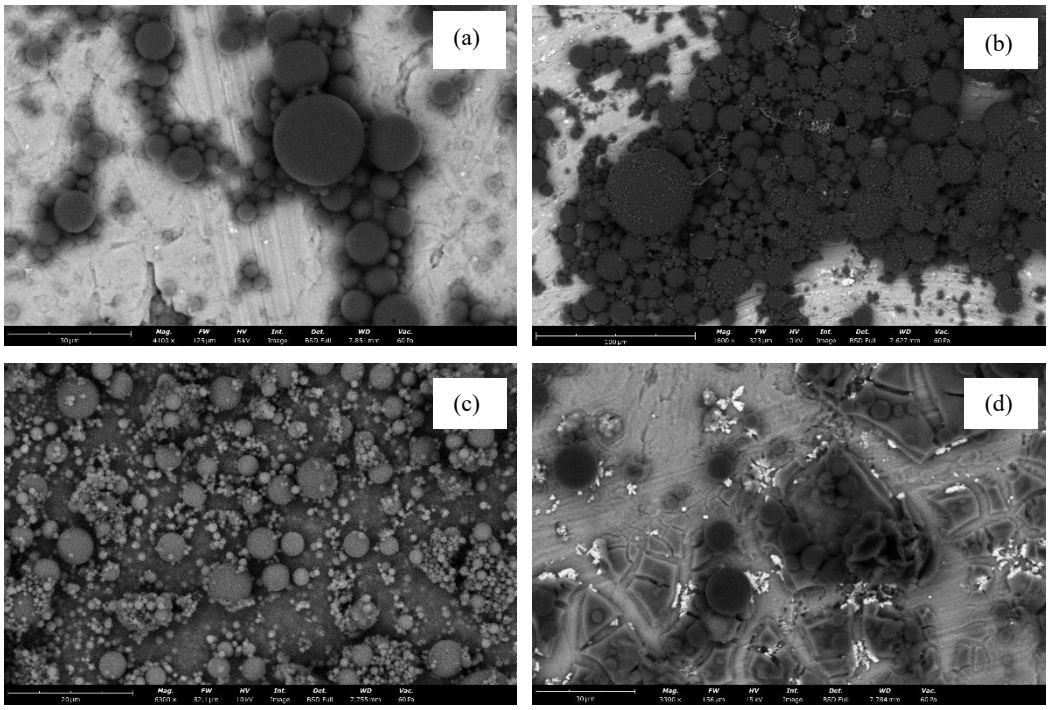

Figure 7. SEM images of PS particles produced by seeded polymerisations in the presence of $NaNO_2$ at different stages of the reaction (a, b, c): (a) to the aqueous medium; (b) dropwise with water; (c) at the very end; and (d) in the presence of $CuCl_2$.

Figure 7 shows SEM images of polystyrene particles produced by seeded polymerisations in the presence of $NaNO_2$ (a, b, c) and $CuCl_2$ (d). In all four cases the presence of several large particles, confirms that the reaction was successful. However, for sodium nitrite, PS particles of approximately 0.50 μm were still produced as byproducts and were observed deposited on the surface of the larger microparticles[24] (Figure 7, b, c) (Dn, 8.17 μm; Dw/Dn, 1.64; Cv, 51 %), indicating that the dispersion remained polydisperse. In the case of the copper chloride, the purification method appeared to be insufficient, as the presence of impurities–potentially unwashed residual starting materials or unremoved copper chloride–were evident in the sample alongside a low particle yield. The reason for this outcome remains unclear.

Since the addition of inhibitors did not achieve in the desired reduction in polydispersity, the next approach focused on modifying and optimizing the purification method. The purification procedure involved centrifugation of the particles followed by subsequent washing. Table 1 summarizes the different solvents, centrifugation times, and speeds that were evaluated in an effort to improve sample uniformity and reduce polydispersity.

Table 1. Centrifugation solvents, speeds and times evaluated as a method of purification.

Solvent	Speed (rpm)	Centrifugal force (xg)	Time (min)	Image number
H_2O	15000	20627	15	a
H_2O	3000	825	10	b
H_2O	1000	91	10	c
EtOH	15000	20627	15	d
EtOH	3000	825	10	e
EtOH	1000	91	10	f
THF	15000	20627	15	-
THF	3000	825	10	-

Figure 8 shows SEM images of the PS particles after being centrifuged and washed with DI water (a, b, c), ethanol (d, e, f) or tetrahydrofuran at specific speeds of 15000 rpm (a, d), 3000 rpm (b, e) or 1000 rpm (c, f).

Among the six conditions from Figure 8, no clear trend or correlation could be established. When DI water was used at 15000 rpm (Figure 8, a) small PS seed particles were still observed between the swollen PS particles. This outcome may be attributed to the high centrifugation speed causing both large and small particles to sediment simultaneously, thus failing to separate them effectively. To attempt better separation of the swollen particles from the seeds, the centrifugation speed was subsequently reduced to 3000 and 1000 rpm. In theory, at these lower speeds, larger particles would sediment while smaller particles would remain suspended, enabling a more selective purification.

However, the SEM images (Figure 8, b, c, d, e) indicate that this theoretical approach was not successful in practice. Despite the reduced speeds with DI water (Figure 8, b, c), small PS particles remained present, and the samples continued to exhibit polydispersity.

When ethanol was used as the washing solvent (Figure 8, d, e, f), additional challenges arose due to the partial solubility of PS in ethanol. This solubility complicated the centrifugation process by risking partial dissolution or aggregation of the particles. The SEM images confirm that ethanol is not an optimal purification solvent, as the particles appear poorly separated, and the polydispersity persists.

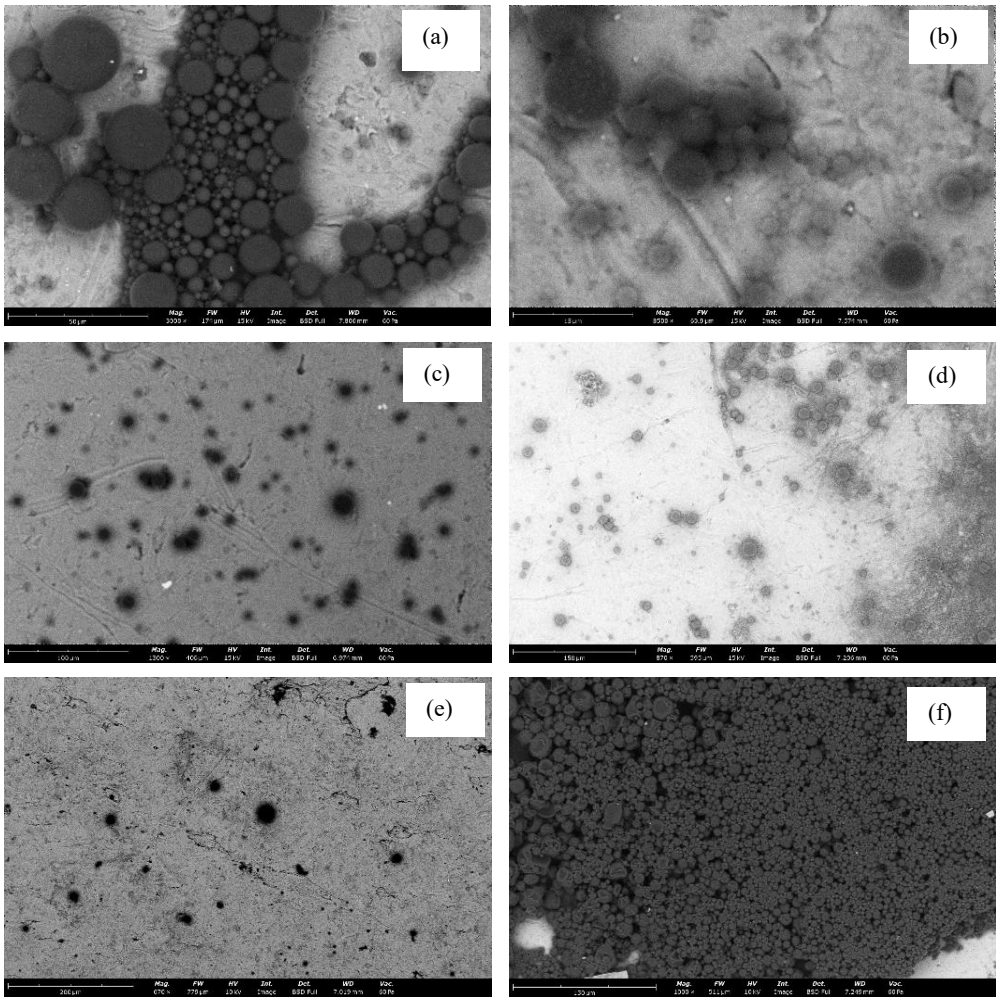

Figure 8. SEM images of the PS particles after being centrifuged and washed with DI water (a, b, c), ethanol (d, e, f) or tetrahydrofuran at specific speeds of 15000 rpm (a, d), 3000 rpm (b, e) or 1000 rpm (c, f).

As none of the previous tested centrifugation solvents proved effective, tetrahydrofuran was subsequently employed based on Xiao et al.[25] article where they reported that small microspheres can be removed by centrifugal washing with THF. However, in this case, centrifugation could not be carried out successfully because PS particles are soluble in the solvent. As a result, it was impossible to maintain a stable dispersion. All attempts to disperse the particles in THF led to their complete dissolution, rendering the purification process ineffective. Consequently, it was not feasible to recover or analyse the particles after treatment with THF.

4.2.2. Infrared analysis

Infrared spectroscopy was carried out on the non-functionalised PS particles–both the seeds and the swollen particles–for multiple purposes. Firstly, it was used to confirm the purity of the polystyrene particles. in the case of the seeds, this analysis also served to detect any residual moisture, which would be indicated by a broad absorption band at around 3300 cm^{-1}

corresponding to the O–H stretching vibrations. Secondly, for the swollen particles, the FT-IR spectra helped to verify that, following the swelling reaction, the chemical composition remained unchanged compared to the seeds, with the only difference being the increased particle size.

Figure 9 shows that the FT-IR spectra of both the seeds and the swollen particles exhibit the same characteristic absorption peaks, indicating no significant change in chemical composition. . The spectra are presented as % of transmittance (ranging between 10 % and 90 %) plotted against wavenumber values from 4000 cm^{-1} to 500 cm^{-1}.

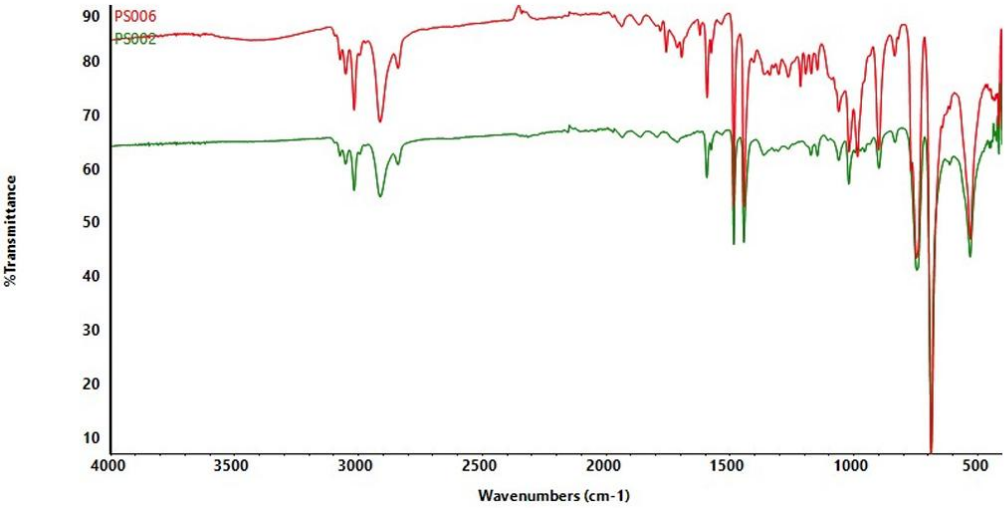

Figure 9. Comparison between the FT-IR spectra of the seed particles (green line) and the FT-IR spectra of the swollen particles (red line).

Absorption peaks at the wavenumbers of 3058 cm^{-1} and 3024 cm^{-1} correspond to aromatic C–H stretching vibrations, while the peaks at 1600 cm^{-1}, 1492 cm^{-1} and 1451 cm^{-1} are characteristic of aromatic C=C stretching vibrations. These peaks confirm the presence of benzene rings within the molecular structures. The absorption peaks at 754 cm^{-1} and 694 cm^{-1} are attributed to the C–H out of plane bending vibrations, indicating that the benzene ring has only a single substituent. Additionally, Figure 9 shows absorption peaks at 2919 cm^{-1} and 2847 cm^{-1}, which correspond to the presence of methylenes ($-CH_2-$) groups.[26]

The peaks observed between 1222 cm^{-1} and 906 cm^{-1} are associated with aromatic ring deformation, specifically in-plane C–H bending, while the peak at 535 cm^{-1} corresponds to the skeletal vibrations involving phenyl ring deformation.

These IR results confirm that styrene has successfully polymerised to form polystyrene, as evidenced by the characteristic absorption bands representative to the polymer's structure. Furthermore, the absence of broad absorption bands around 3300 cm^{-1} indicates negligible water or moisture content in the samples. Finally, the comparative analysis of the spectra from both the

seed and swollen particles confirms that their chemical compositions remain consistent, with the only notable difference being an increase in particle size.

4.3. Functionalisation of the seeds by using UV light

4.3.1. Size and morphology analysis

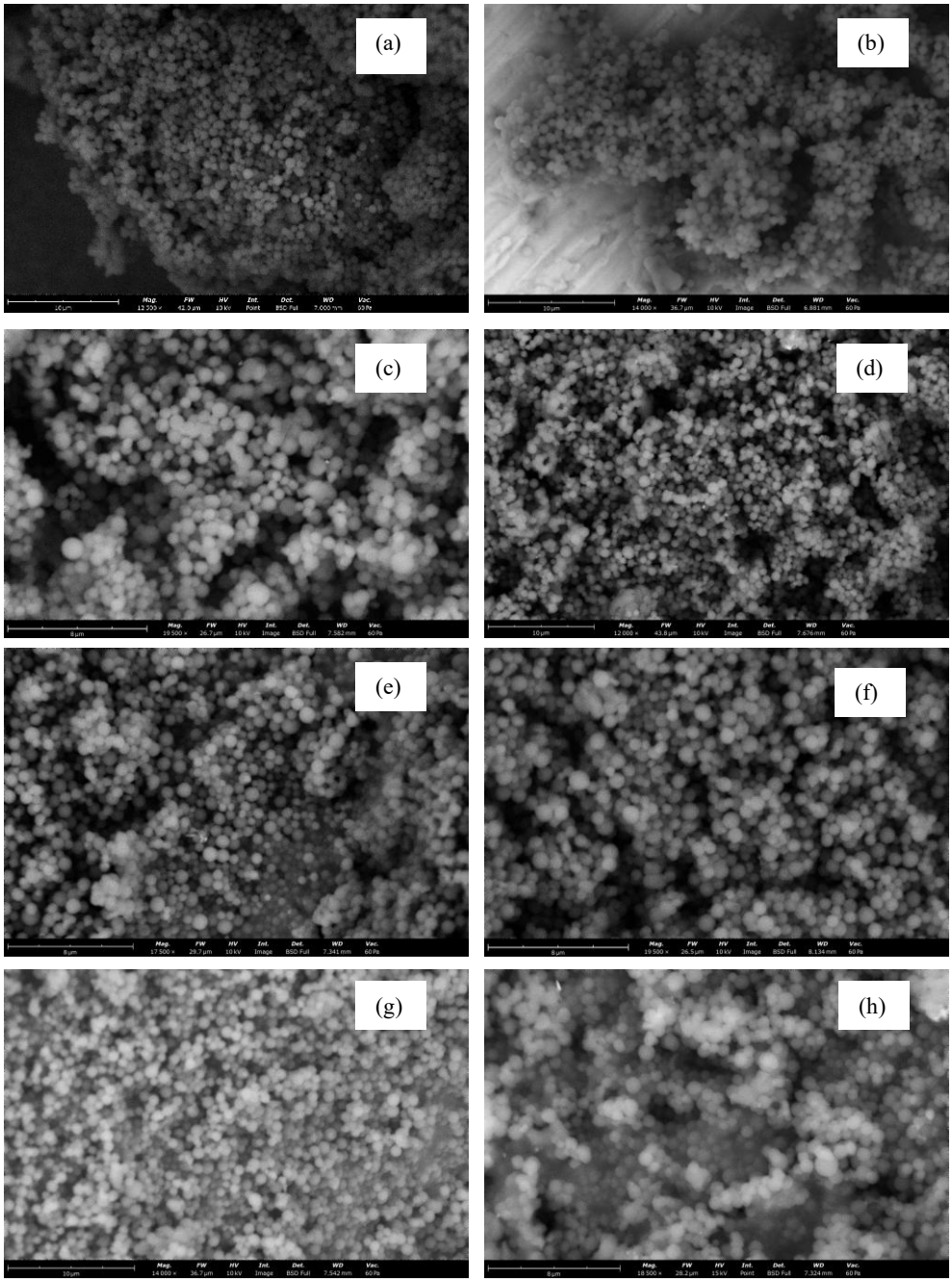

Figure 10. SEM images of PS seeds after being treated by different UV irradiation times: (a) 0 hours; (b) 2 hours; (c) 4 hours; (d) 8 hours; (e) 24 hours; (f) 48 hours; (g) 96 hours; (h) 120 hours.

Pristine polystyrene particles are typically uniform, smooth spheres. However, when exposed to ageing processes, their surfaces develop pores and become increasingly rough.[21] To investigate the effect of UV radiation on the surface morphology of the PS particles, SEM analysis was conducted. Figure 10 presents SEM images of PS following exposure to UV irradiation for varying durations: (a) 0 hours; (b) 2 hours; (c) 4 hours; (d) 8 hours; (e) 24 hours; (f) 48 hours; (g) 96 hours; (h) 120 hours.

As shown in Figure 9, the hypothesis presented at the beginning of this section was not confirmed as all SEM images demonstrate that the PS seed particles maintained their spherical morphology regardless of the UV exposure duration. However, the surface characteristics were not thoroughly resolved in these images due to limitations in SEM resolution caused by surface charging effects under the electron beam. To better characterise the particle surfaces, further improvements in sample preparation are needed, such as coating the particles with a conductive layer like gold or preparing a monolayer of particles to reduce charging and enhance image quality. Additionally, the relatively short irradiation times and the low energy of the lamp (365 nm) used here may have been insufficient to induce morphological changes. Longer UV exposure and higher energy lamp (254 nm) on the order of one to three months, as reported by Mao et al.[21] might result in surface modifications such as roughening or loss of smoothness.

4.3.2. Infrared analysis

Infrared spectroscopy was performed to the functionalised polystyrene particles to study the effect of UV irradiation on their chemical composition. Several times of exposure (0 hours; 2 hours; 4 hours; 8 hours; 24 hours; 48 hours; 96 hours and 120 hours) to UV light were tested based on the expectation that the intensity of peaks corresponding to oxygen-containing functional groups would increase with increasing aging time.[21] However, the trend of variations in the FT-IR absorption peaks of PS is observed to have consistent patterns across all irradiation times.

Moreover, conventional FT-IR instruments detect signals from the bulk of the sample so if the functionalisation is only present in the surface of the particles, which is the case of this experiment, the intensity of the peaks is expected to have reduced values or they can even overlap with the dominant signals of the unmodified polystyrene, limiting then the detectability of the modifications.

Both these outcomes may be attributed to the short irradiation times used in this study. Had the particles been exposed to UV radiation for longer periods, i.e. one or three months, like Mao et al.[21] reported, a more pronounced differentiation in the FT-IR peak intensities of the distinct irradiation times would likely have been observed. Furthermore, the overall intensity values of

the oxygen-containing functional groups would be expected to increase significantly under prolongated irradiation.

By comparing the absorption peaks of PS before (Figure 9) and after (Figure 11) aging, it can be observed that the characteristic backbone signal of polystyrene remain present. The peaks at 3059 cm^{-1} and 3014 cm^{-1} correspond to aromatic C–H stretching vibration absorption, while peaks at 1602 cm^{-1}, 1495 cm^{-1} and 1457 cm^{-1} are characteristic of aromatic C=C stretching vibrations, all of which confirm the presence of benzene rings in the structure. The absorption peaks at 744 cm^{-1} and 684 cm^{-1} correspond to the C–H out-of-plane bending vibrations, indicating that the benzene ring is mono-substituted.

Additional peaks seen in between 1223 cm^{-1} and 908 cm^{-1} arise from aromatic ring deformation and in-plane C-H bending, while the peak at 537 cm^{-1} corresponds to skeletal vibrations related to phenyl ring deformation. These findings confirm that the core structure of the polymer remain polystyrene even after UV exposure.

Figure 11 presents the FT-IR spectra of both pristine and functionalised particles across the various exposure (0 hours; 2 hours; 4 hours; 8 hours; 24 hours; 48 hours; 96 hours; 120 hours). The spectra are displayed as %Transmittance (ranging between 55 % and 90 %) versus wavenumber values (from 4000 cm^{-1} to 500 cm^{-1}).

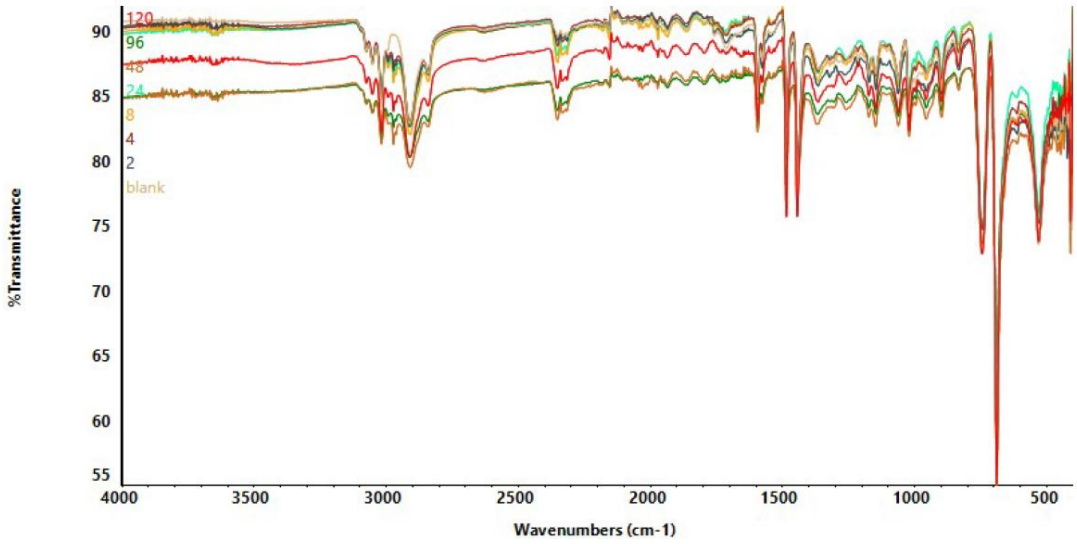

Figure 11. FT-IR spectra of PS, treated by different irradiation times: 0 hours; 2 hours; 4 hours; 8 hours; 24 hours; 48 hours; 96 hours; 120 hours.

After irradiation, some changes can be observed over the whole IR spectrum, attributed to the formation of suspected oxidation products, as illustrated in Figure 12, following the predicted reaction mechanism from Scheme 8.

Figure 12 illustrates the molecular structures of polystyrene and its UV-induced oxidation products. The pristine **PS** molecule, which has not been subjected to irradiation, retains the characteristic PS core structure, consisting of a benzene ring and an aliphatic methylene backbone. In contrast, the irradiated derivatives maintain this same polystyrene backbone but display distinct functional modifications that facilitate their identification in the FT-IR spectra. Specifically, molecule **1** corresponds to a hydroperoxide, molecule **2** to an aldehyde, and molecule **3** to an alcohol. These oxygen-containing functional groups introduce new or shifted absorption bands within the infrared region, reflecting the chemical alterations induced by UV exposure.

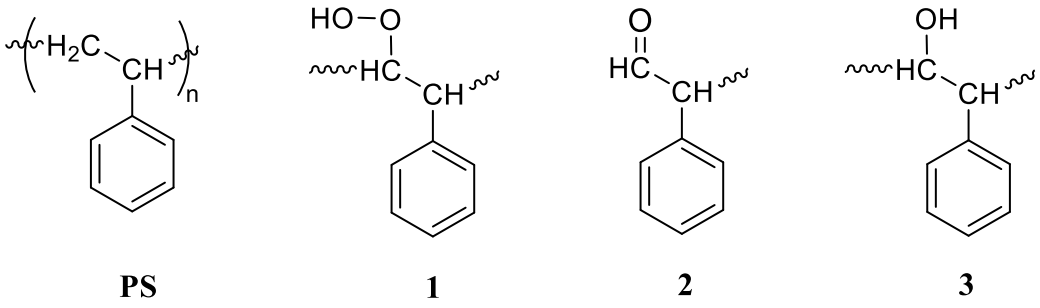

Figure 12. Raw polystyrene and oxidation products. PS) pristine 1) hydroperoxide; 2) aldehyde; 3) alcohol.

The first and most notable change observed in the FT-IR spectra is the appearance of the absorption peak at around 2970 cm^{-1} in all UV-irradiated samples, which is absent in the non-irradiated (blank) sample. This peak is characteristic of C–H stretching vibrations in methyne (–CH–) groups. As illustrated in Figure 12, the pristine molecule contains both methylene and methyne groups in the backbone of the structure, whereas the irradiated derivatives, (compounds **1**, **2** and **3**) primarily feature methyne functionalities.

The increased intensity of the 2970 cm^{-1} absorption band in the functionalised samples, compared to the pristine polystyrene, can thus be attributed to the higher concentration of methyne groups generated through UV-induced chemical transformations.

Another important change that can be observed in the spectra of the functionalised particles is the emerge of a new band at around 3600 cm^{-1}. This peak, typically broad and prominent, corresponds to O–H stretching vibrations and can be attributed to the formation of hydroxyl-containing species, such as compounds **1** and **3** in Figure 12, which are generated following UV irradiation. The absence of this band in the pristine sample further confirms that UV exposure leads to chemical modification of the particles.

The relatively low intensity of this peak is likely due to the relatively short irradiation times used in this study. Prolonged exposure would be expected to yield a more pronounced and broader

absorption band in this region, reflecting an increased formation of hydroxyl groups over extended irradiation periods.

Therefore, the presence of these two characteristic bands in the FT-IR spectra (the C–H stretching band at 2970 cm^{-1} and the O–H stretching band around 3600 cm^{-1}) observed in the functionalised polystyrene samples but absent in the pristine one, provides clear evidence that the particles have undergone chemical modification after the UV aging. Although the intensities of these bands remain relatively low, likely due to short irradiation times, their appearance nonetheless confirms that the functionalisation has occurred to some extent.

The identification of additional characteristic peaks corresponding to newly introduced functional groups in the aged products is more challenging, as many of these signals either overlap with existing polystyrene bands or are present at low intensity. Nevertheless, some of these peaks can still be observed.

At approximately 1000 cm^{-1}, a subtle peak is visible, which corresponds to the O–O stretching vibration present in compound **1**. However, this signal partially overlaps with the in-plane C–H bending vibration of the aromatic ring deformation, making it difficult to fully resolve. Near 1700 cm^{-1}, a characteristic peak attributed to the C=O stretching vibration appears, corresponding to the aldehyde group present in compound **2**. Additionally, a small band is observed at around 1350 cm^{-1}, which corresponds to the C–OH stretching vibration of the phenolic hydroxyl group unique to compound **3**. The overall low intensity of these bands can be explained by the fact that each functional group appears in only one of the three oxidised products.

Furthermore, a weak band is detected at approximately 1050 cm^{-1}, which corresponds to the C–O bond stretching vibration present in both compounds **1** and **3**, though this band also partially overlaps with the in-plane C–H bending of the aromatic ring.

An additional peak appears near 2350 cm^{-1}; however, this absorption does not arise from any vibrations within the sample itself but is attributed to atmospheric carbon dioxide. Gaseous CO_2 exhibits a characteristic doublet in this region even at ambient concentrations of around 350 ppm.

For clarity, Table 2 summarises the FT-IR peak assignments discussed above, listing the approximate band positions, the corresponding vibrational modes, and the associated compounds from Figure 12.

Table 2. FT-IR band assignment summary.

Band value (cm^{-1})	Assigned bond	Compound number [a]
≃ 2970	ν(C–H)	1, 2, 3
≃ 3600	ν(O–H)	1, 3
≃ 1000	ν(O–O)	1
≃ 1700	ν(C=O)	2
≃ 1350	ν(C–OH)	3
≃ 1050	ν(C–O)	1, 3
≃ 2350	atm. CO_2	-

a. Compound number refers to the functionalisation products shown in Figure 12.

All the observations commented above confirm that, despite the low signal intensity and limited amount of functionalisation products, their presence is detectable, therefore, it corroborates that the functionalisation process was successful.

In order to gain a more comprehensive understanding of the chemical modifications occurring during the UV-induced aging of the PS particles, it is recommended to conduct further characterisation using nuclear magnetic resonance (NMR) spectroscopy. NMR would enable more precise identification of the newly formed functional groups and allow for the structural elucidation of the functionalised products. Additionally, it would facilitate the quantification of the different functionalisation products within the mixture and permit monitoring of the reaction progress over time, thereby providing valuable insight into the formation and evolution of the predominant products at various stages of UV exposure.

4.4. Uniformity and coefficient of variation calculation

To study the polydispersity of the samples, that is, to evaluate how similar the particles are in size, the uniformity and the coefficient of variation were calculated for both the PS seed particles and all subsequent swelling attempts.

The number-average diameter (D_n), the weight-average diameter (D_w) and the coefficient of variation (C_v) of the diameter of the particles were calculated by using equations (1), (2)[27] and (3) respectively. The calculations were done by counting at least 100 individual particles from the SEM images.

$$D_n = \frac{\sum n_i\, d_i}{n_T} \quad (1)$$

$$D_w = \frac{\sum {d_i}^3}{\sum {d_i}^2} \quad (2)$$

$$Uniformity = \frac{D_w}{D_n} \quad (3)$$

$$C_v = \frac{\sigma}{\mu} \times 100 \quad (4)$$

Where n_i is the number of particles, d_i is the specific diameter of particle *i,* n_T is the total number of particles and uniformity is the ratio between D_w and D_n. For the C_v calculation it was taken the standard deviation (σ) and the mean value (μ) of all the data.

Table 3. Values for the primary size, the uniformity and the coefficient of variation of different PS samples.

Sample	Primary size (μm)	Uniformity	C_v (%)
Seeds	0.97	1.08	11.7
Swelling (1)	8.21	1.74	58.6
Swelling (2)	8.17	1.64	51.0
Swelling (3)	6.12	2.43	83.8
Swelling (4)	3.45	1.47	49.9
Swelling (5)	5.47	1.46	45.5

Swelling product: (1) styrene dispersion, without inhibitor; (2) $NaNO_2$ inhibitor, added to the aqueous medium; (3) $NaNO_2$ inhibitor, added dropwise with water; (4) $NaNO_2$ inhibitor, added at the end; (5) $CuCl_2$ inhibitor.

The primary size, the uniformity and the coefficient of variation of the different PS samples are summarised in Table 3. For the seed samples, measurements were taken from 200 individual particles observed in the SEM images (Figure 3) as the high particle density in the photographs allowed a more statistically reliable analysis. While for the swollen particles only 100 particle measurements were taken due to the significantly lower reaction yield, which resulted in a much more reduced number of observable particles.

The particle size measurements obtained by SEM analysis, demonstrate and confirm that the seeds reaction was successful as the average particle size is of 0.97 μm. On the other hand, the measurements for the swollen samples exhibit greater variability because all of them still contain small PS particles.

In the case of the swelling (4), the SEM image (Figure 7, c) clearly shows the presence of swollen particles, however, a significant proportion of smaller PS particles, of about 0.50 μm in diameter, were still byproduced in the surface of the big microparticles. This broad size distribution led to

a decrease in the overall average particle size, resulting in a value of 3.45 μm, which is considerably lower than those typically expected from a successful swelling process. In contrast, although swelling samples (1), (2) and (3) also contained both large and small particles (Figure 6, Figure 7, a and b, respectively), the measurements obtained (8.21 μm, 8.17 μm and 6.12 μm, respectively) are considered more accurate due to the reduced presence of smaller particles. For the swelling (5), as the SEM image shows (Figure 7, d) the purification method does not appear to have been fully effective given the presence of impurities in the sample. These impurities likely contributed to a reduction in the particle yield and may have caused overlapping with the actual particles.

The uniformity calculation from the seeds shows that the particle size distribution is fairly monodisperse and well-defined as the value obtained for the ratio between the number-average diameter (D_n) and the weight-average diameter (D_w) is of 1.08. A uniformity value approaching to 1 signifies a high degree of monodispersity, as it implies the minimal variation between D_n and D_w, indicating that the particle sizes are regularly distributed.

The swelling (3) exhibited the highest uniformity value of 2.43, indicating the greatest degree of polydispersity among the samples. This elevated value may be due to the fact that in the SEM photographs from this swelling reaction (Figure 7, b), there were exceptionally large particles measuring up to 23.77 μm, which may potentially have influenced in the calculation of the uniformity.

Among the remaining swelling samples, the calculated values are relatively similar, indicating a moderate degree of polydispersity. While these samples do not exhibit the high uniformity observed in the seed particles, again likely due to the presence of smaller particles seen in the SEM images, their uniformity value does not increase drastically.

A similar trend is observed in the coefficient of variation calculations. The value obtained for the seed particles again indicates a fairly monodisperse size distribution, with only 11.7 % of variation. In general, a lower C_v value corresponds to a higher degree of monodispersity, as it reflects minimal variation in particle diameters.

The same behaviour happens for the swelling (3), in which it has been obtained a C_v of 83.8 %, again probably due to the existence of the exceptionally large particles present in the sample (Figure 7, b). And, finally, the remaining swelling samples exhibit moderate values, suggesting a relatively broad size distribution and confirming that the degree of polydispersity is not negligible.

In summary of all the above information, it can be concluded that the seed synthesis successfully yielded polystyrene particles with a high degree of monodispersity. However, despite the fact that all swelling attempts, for which the calculations were performed, produced swollen particles with

diameters of around 10 μm, the overall monodispersity of these samples remains limited due to the coincident formation of smaller PS particles.

5. Conclusions

The conventional synthesis route of polystyrene microspheres of 1µm and 10 µm was modified by employing benzoyl peroxide (BPO) as initiator in both polymerisation steps, rather than using 2,2'-azobisisobutyronitrile (AIBN) in the first step and BPO in the second, as typically reported in the literature. The synthesis was successfully carried out via chain-growth free-radical dispersion polymerisation.

The first objective of this work was effectively achieved as seed particles were successfully synthesized with a high degree of monodispersity. The second objective was also fulfilled as the seed particles effectively absorbed sufficient styrene monomer during the swelling step, resulting in the formation of solid polystyrene microspheres with diameters of approximately 10 µm after polymerisation.

The third objective, which aimed to reduce the polydispersity of the swollen particles by supressing the formation of new secondary PS microspheres, was only partially successful. Despite multiple optimisation attempts and modifications of the synthetic protocol, polydispersity remained significant, as small polystyrene microparticles continued to form, either adhering to the surface of the larger spheres or present as independent particles dispersed in the medium.

The final objective was to expose the seed particles to UV irradiation in order to generate model particles with functionalised surfaces suitable for carbon isotope exchange (CIE) radiolabelling. Based on the post-irradiation characterisation results, it can be concluded that functionalisation was achieved. FT-IR spectra revealed the emergence of characteristic peaks corresponding to oxygen-containing functional groups introduced by the UV-induced surface oxidation. However, as the FT-IR peak intensities remained relatively low and the SEM images showed no visible changes in the particle morphology, it is inferred that only a limited degree of functionalisation was achieved under the present experimental conditions.

For future optimisation, extending the UV irradiation times or exploring alternative irradiation wavelengths could enhance the degree of surface functionalisation. The next stage of this research will involve applying radiolabelling techniques to the functionalised polystyrene microspheres. This will enable their application as model particles for advanced analytical studies, including tracing, quantification, and environmental or biological fate assessments in complex systems.

Conclusions

El mètode de síntesi convencional de microesferes de poliestirè d'1 µm i 10 µm ha estat modificat tot emprant peròxid de benzoïl (BPO) com a iniciador en ambdós passos de la polimerització, en lloc d'utilitzar 2,2'-azobis(isobutironitril) (AIBN) en el primer pas i BPO en el segon, com es reporta habitualment. La síntesi es va dur a terme amb èxit mitjançant una polimerització en dispersió per radicals lliures per creixement en cadena.

El primer objectiu d'aquest treball ha estat assolit correctament, ja que s'han sintetitzat partícules "seed" de manera eficient, tot mostrant un alt grau de monodispersitat. El segon objectiu també s'ha acomplert, ja que les partícules "seed" van absorbir suficient monòmer d'estirè durant el procés d'inflament, resultant en la formació de partícules sòlides de poliestirè amb diàmetres d'aproximadament 10 µm després de la polimerització.

El tercer objectiu ha estat reduir la polidispersitat de les partícules inflades tot prevenint la formació de noves microesferes de PS. No obstant això, malgrat diversos intents i modificacions dels mètodes ja existents, la polidispersitat es va mantenir similar per a les partícules inflades, ja que petites micropartícules de poliestirè continuaven formant-se, ja sigui adherides a la superfície de les partícules més grans o apareixent de manera independent dins del medi.

Finalment, l'últim objectiu va ser sotmetre les partícules "seed" a llum ultraviolada (UV) per intentar produir partícules model amb superfícies funcionalitzades per preparar l'intercanvi d'isòtops de carboni (CIE) per radiomarcatge. A través dels resultats de caracterització obtinguts després de la irradiació, es pot concloure que la funcionalització ha estat exitosa, ja que els espectres FT-IR mostren pics característics corresponents a grups funcionals que contenen oxigen induïts a la superfície del poliestirè. Tot i la baixa intensitat dels pics de l'espectre FT-IR i les esferes aparentment no modificades que es poden observar a les imatges SEM, es suggereix que només s'ha format una petita quantitat de producte funcionalitzat, sota les condicions experimentals emprades.

Per tant, una possible direcció per a futurs treballs seria ampliar el temps d'irradiació UV, és a dir, deixar les partícules sota l'efecte de la llum durant períodes de temps més llargs, per millorar la funcionalització.

Per seguir avançant en aquesta línia de recerca, el següent pas seria sotmetre les partícules de poliestirè funcionalitzades als procediments de radiomarcatge. Això permetrà la seva aplicació en una gran varietat de tècniques analítiques, especialment per a seguiment, quantificació o estudis en sistemes ambientals i biològics complexos.

6. Bibliography

(1) Saldivar-Guerra, Enrique.; Vivaldo-Lima, Eduardo. *Handbook of Polymer Synthesis, Characterization, and Processing*; Wiley, 2013 pp 3.

(2) Brown Tyson; Gabrielli André; Borgia Gina; *Microplastics*. National Geographic Society. https://education.nationalgeographic.org/resource/microplastics/.

(3) Tirkey, A.; Upadhyay, Microplastics: An Overview on Separation, Identification and Characterization of Microplastics. **2021**. https://doi.org/10.1016/j.marpolbul.2021.112604.

(4) Lim, X. Microplastics Are Everywhere — but Are They Harmful? *Nature* **2021**, *593* (7857), 22–25. https://doi.org/10.1038/d41586-021-01143-3.

(5) Roslan, N. S.; Lee, Y. Y.; Ibrahim, Y. S.; Tuan Anuar, S.; Yusof, K. M. K. K.; Lai, L. A.; Brentnall, T. Detection of Microplastics in Human Tissues and Organs: A Scoping Review. *J. Glob. Health* **2024**, *14*, 04179. https://doi.org/10.7189/jogh.14.04179.

(6) Millican, J. M.; Agarwal, S. Plastic Pollution: A Material Problem? *Macromolecules* **2021**, *54* (10), 4455–4469. https://doi.org/10.1021/acs.macromol.0c02814.

(7) Ribeiro, A. P. C.; Martins, M. O.; Figueiras, A. O.; Martins. Introduction to Polymerization and Depolymerization; 2025; pp 1–23. https://doi.org/10.1021/bk-2025-1498.ch001.

(8) Kim, J.; Suh, K. Monodisperse Micron-Sized Polystyrene Particles by Seeded Polymerization: Effect of Seed Crosslinking on Monomer Swelling and Particle Morphology. *Polymer* **2000**, *41*, 6181–6188. https://doi.org/10.1016/S0032-3861(99)00846-0.

(9) Kloust, H.; Pöselt, E.; Kappen, S.; Schmidtke, C.; Kornowski, A.; Pauer, W.; Moritz, H.; Weller, H. Ultrasmall Biocompatible Nanocomposites: A New Approach Using Seeded Emulsion Polymerization for the Encapsulation of Nanocrystals. *Langmuir* **2012**, *28* (18), 7276–7281. https://doi.org/10.1021/la300231r.

(10) Okubo, M.; Shiozaki, M.; Tsujihiro, M.; Tsukuda, Y. Preparation of Micron-Size Monodisperse Polymer Particles by Seeded Polymerization Utilizing the Dynamic Monomer Swelling Method. *Colloid. Polym. Sci.* **1991**, *269* (3), 222–226. https://doi.org/10.1007/BF00665495.

(11) Li, W.; Pham, H. H.; Nie, Z.; MacDonald, B.; Güenther, A.; Kumacheva, E. Multi-Step Microfluidic Polymerization Reactions Conducted in Droplets: The Internal Trigger Approach. *J. Am. Chem. Soc.* **2008**, *130* (30), 9935–9941. https://doi.org/10.1021/ja8029174.

(12) Yan, Q.; Bai, Y.; Meng, Z.; Yang, W. Precipitation Polymerization in Acetic Acid: Synthesis of Monodisperse Cross-Linked Poly(Divinylbenzene) Microspheres. *J. Phys. Chem. B* **2008**, *112* (23), 6914–6922. https://doi.org/10.1021/jp711324a.

(13) Wang, D.; Yu, B.; Cong, H.; Wang, Y.; Wu, Q.; Wang, J. Synthesis of Monodisperse Polystyrene Microspheres by Seeding Polymerization. *Integr. Ferroelectr.* **2013**, *147* (1), 41–46. https://doi.org/10.1080/10584587.2013.790287.

(14) Ugelstad, J.; Mfutakamba, H. R.; Mørk, P. C.; Ellingsen, T.; Berge, A.; Schmid, R.; Holm, L.; Jørgedal, A.; Hansen, F. K.; Nustad, K. Preparation and Application of Monodisperse Polymer Particles. *J. Polym. Sci.: Polymer Symposia* **1985**, *72* (1), 225–240. https://doi.org/10.1002/polc.5070720125.

(15) Al-Sid-Cheikh, M.; Rowland, S. J.; Kaegi, R.; Henry, T. B.; Cormier, M.; Thompson, R. C. Synthesis of ^{14}C-Labelled Polystyrene Nanoplastics for Environmental Studies. *Commun. Mater.* **2020**, *1* (1), 97. https://doi.org/10.1038/s43246-020-00097-9.

(16) Wuliji, H.; Zhao, K.; Jing, H.; Ouyang, R.; Yang, Y.; Wei, T. R.; Zhu, H.; Shi, X. Defect Chemistry for Extrinsic Doping in Ductile Semiconductor α-Ag_2S. *J. Mater.* **2024**, *10* (6), 1270–1278. https://doi.org/10.1016/j.jmat.2024.01.009.

(17) Chapman, S.; Oparka, K. J.; Roberts, A. G. New Tools for in Vivo Fluorescence Tagging. *Curr. Opin. Plant. Biol.* **2005**, *8* (6), 565–573. https://doi.org/10.1016/j.pbi.2005.09.011.

(18) Kopf, S.; Bourriquen, F.; Li, W.; Neumann, H.; Junge, K.; Beller, M. Recent Developments for the Deuterium and Tritium Labeling of Organic Molecules. *Chem. Rev.* **2022**, *122* (6), 6634–6718. https://doi.org/10.1021/acs.chemrev.1c00795.

(19) Gauthier, D. R.; Rivera, N. R.; Yang, H.; Schultz, D. M.; Shultz, C. S. Palladium-Catalyzed Carbon Isotope Exchange on Aliphatic and Benzoic Acid Chlorides. *J. Am. Chem. Soc.* **2018**, *140* (46), 15596–15600. https://doi.org/10.1021/jacs.8b09808.

(20) Fred W. Billmeyer. *Textbook of Polymer Science*, 3rd ed.; Ilustrada, Ed.; John Wiley & Sons., 1984; Vol. 1. pp 52.

(21) Mao, R.; Lang, M.; Yu, X.; Wu, R.; Yang, X.; Guo, X. Aging Mechanism of Microplastics with UV Irradiation and Its Effects on the Adsorption of Heavy Metals. *J. Hazard. Mater.* **2020**, *393*, 122515. https://doi.org/10.1016/j.jhazmat.2020.122515.

(22) Yousif, E.; Haddad, R. Photodegradation and Photostabilization of Polymers, Especially Polystyrene: Review. *SpringerPlus* **2013**, *2*, 398. https://doi.org/10.1186/2193-1801-2-398.

(23) Wang, X.; Wu, P. Preparation of Highly Thermally Conductive Polymer Composite at Low Filler Content via a Self-Assembly Process between Polystyrene Microspheres and Boron Nitride Nanosheets. Supporting Information. *ACS. Appl. Mater. Interfaces.* **2017**, *9* (23), 19934–19944. https://doi.org/10.1021/acsami.7b04768.

(24) Okubo, M.; Ise, E.; Yamashita, T. Production of Micron-Sized Monodispersed Polymer Particles by Seeded Polymerization for the Dispersion of Highly Monomer-Swollen Particles Prepared with Submicron-Sized Polymer Seed Particles Utilizing the Dynamic Swelling Method. *J. Polym. Sci. A. Polym. Chem.* **1998**, *36*, 2513–2519. https://doi.org/10.1002/(SICI)1099-0518(199810)36:14<2513::AID-POLA10>3.0.CO;2-L.

(25) Xiao, J.; Cao, H.; Cong, H.; Shen, Y.; Yu, B. Preparation and Modification of Monodisperse Large Particle Size Crosslinked Polystyrene Microspheres and Their Application in High Performance Liquid Chromatography. *React. Funct. Polym.* **2022**, *178*, 105357. https://doi.org/10.1016/j.reactfunctpolym.2022.105357.

(26) Fang, J.; Xuan, Y.; Li, Q. Preparation of Polystyrene Spheres in Different Particle Sizes and Assembly of the PS Colloidal Crystals. *Sci. China. Technol. Sci.* **2010**, *53* (11), 3088–3093. https://doi.org/10.1007/s11431-010-4110-5.

(27) Han, H.; Lee, J.; Hong, J.; Shim, S. E. Dispersion Polymerization of Styrene Employing Lyophilic Comonomer in the Absence of Stabilizer: Synthesis of Impurity-Free Microspheres. *Macromol. Res.* **2009**, *17* (7), 469–475. https://doi.org/10.1007/BF03218894.